



저작자표시-비영리-변경금지 2.0 대한민국

이용자는 아래의 조건을 따르는 경우에 한하여 자유롭게

- 이 저작물을 복제, 배포, 전송, 전시, 공연 및 방송할 수 있습니다.

다음과 같은 조건을 따라야 합니다:



저작자표시. 귀하는 원저작자를 표시하여야 합니다.



비영리. 귀하는 이 저작물을 영리 목적으로 이용할 수 없습니다.



변경금지. 귀하는 이 저작물을 개작, 변형 또는 가공할 수 없습니다.

- 귀하는, 이 저작물의 재이용이나 배포의 경우, 이 저작물에 적용된 이용허락조건을 명확하게 나타내어야 합니다.
- 저작권자로부터 별도의 허가를 받으면 이러한 조건들은 적용되지 않습니다.

저작권법에 따른 이용자의 권리는 위의 내용에 의하여 영향을 받지 않습니다.

이것은 [이용허락규약\(Legal Code\)](#)을 이해하기 쉽게 요약한 것입니다.

[Disclaimer](#)

공학석사학위논문

**Improvement of SBAS ionospheric
correction generation using Chapman
electron density distribution**

**Chapman 전자 밀도 분포를 이용한
SBAS 전리층 보정 정보 정확도 개선**

2019년 2월

서울대학교 대학원

기계항공공학부

최 봉 관

Abstract

Improvement of SBAS ionospheric correction generation using Chapman electron density distribution

Bongkwan Choi

School of Mechanical and Aerospace Engineering

The Graduate School

Seoul National University

Satellite Based Augmentation System (SBAS) gives ionospheric correction data to Global Navigation Satellite System (GNSS) users to make users can estimate their position more accurately. To generate the ionospheric correction data, reference stations of SBAS estimate vertical ionospheric delay at Ionospheric Pierce Point (IPP) from slant ionospheric delay by using obliquity factor of thin shell model. However, obliquity factor depends only on the elevation angle of satellites. As a result, vertical ionospheric delay can be estimated inaccurately when the thin shell model is used and it finally occurs the error in the ionospheric correction data.

This paper proposed a method to estimate the vertical delay from the slant delay, which can improve accuracy of the ionospheric correction of SBAS. Proposed method used Chapman profile which is a model for the vertical electron density distribution of the

ionosphere. In the proposed method, we assumed that parameters of Chapman profile are given and the vertical ionospheric can be modeled with linear function. We also divided ionosphere into multi-layer.

For the verification, we converted slant ionospheric delays to vertical ionospheric delays by using the proposed method and generated the ionospheric correction of SBAS with vertical delays. We used International Reference Ionosphere (IRI) model for the simulation to verification. As a result, the accuracy of ionospheric correction from proposed method has been improved for 17.3% in daytime, 10.2% in evening, 2.1% in nighttime, compared with correction from thin shell model. Finally, we verified the method in the SBAS user domain, by comparing slant ionospheric delays of users. Using the proposed method, root mean square value of slant delay error decreased for 23.6% and max error value decreased for 27.2%.

Key words : SBAS, ionospheric correction, Chapman profile, ionospheric delay, IRI

Student number : 2017–20877

Contents

ABSTRACT	I
CONTENTS.....	III
LIST OF FIGURES	V
LIST OF TABLES.....	VII
I. INTRODUCTION	1
1. <i>Motivation and Objective</i>	<i>1</i>
2. <i>Trends of Research</i>	<i>2</i>
3. <i>Research Contents and Method</i>	<i>4</i>
4. <i>Contribution</i>	<i>5</i>
II. CURRENT PROCESS OF SBAS IONOSPHERIC CORRECTION	7
III. PROPOSED METHOD FOR GENERATION OF SBAS IONOSPHERIC CORRECTION	11
1. <i>Introduction of Chapman profile.....</i>	<i>12</i>
2. <i>Introduction of Hoque's algorithm.....</i>	<i>13</i>
3. <i>Assumptions used in the proposed method.....</i>	<i>16</i>
4. <i>Development of the algorithm.....</i>	<i>18</i>
IV. VERIFICATION OF THE PROPOSED METHOD	24
1. <i>Simulation for the verification</i>	<i>24</i>
2. <i>Verification in SBAS ionospheric correction domain</i>	<i>29</i>
3. <i>Verification in SBAS user domain.....</i>	<i>39</i>

V. CONCLUSION	44
REFERENCE	46
초 록	48

List of Figures

FIGURE II-I CONCEPTUAL FIGURE OF SBAS	7
FIGURE II-II IGP DEFINED IN MOPS.....	8
FIGURE II-III SBAS USER ALGORITHM OF IONOSPHERIC CORRECTION	9
FIGURE II-IV SBAS IONOSPHERIC CORRECTION PROCESS WITH THE PROPOSED METHOD	10
FIGURE III-I CONCEPTUAL FIGURE OF THE PROPOSED METHOD.....	11
FIGURE III-II CHAPMAN PROFILE AND TRUE ELECTRON DENSITY DISTRIBUTION OF IONOSPHERE.....	12
FIGURE III-III CONCEPTUAL FIGURE OF THE HOQUE’S ALGORITHM	14
FIGURE III-IV ASSUMPTIONS USED IN THE PROPOSED METHOD	17
NOW, WE WILL EXPLAIN THE PROPOSED ALGORITHM. THE PROPOSED ALGORITHM IS SHOWN THROUGH FIGURE III-V THROUGH III-VI.....	18
FIGURE III-VII ALGORITHM OF THE PROPOSED METHOD 1	19
FIGURE III-VIII ALGORITHM OF THE PROPOSED METHOD 2.....	19
FIGURE III-IX ALGORITHM OF THE PROPOSED METHOD 3.....	20
FIGURE III-X DERIVATION OF I^{TH} OBLIQUITY FACTOR.....	22
FIGURE IV-I HISTOGRAM OF Kp INDEX (1932.01.01 ~ 2017.12.31)	25
FIGURE IV-II VERTICAL IONOSPHERIC DELAY (M) AROUND KOREA ON 2011.06.20 KST (UPPER : 14HR, MIDDLE : 18HR, LOWER : 23HR).....	27
FIGURE IV-III PLANNED LOCATION OF THE REFERENCE STATIONS OF KASS.....	28
FIGURE IV-IV ESTIMATION ERROR AT IPP (DATE : 2011.06.20 23HR)	30
FIGURE IV-V IGP ESTIMATION RESULT OF IPP DATA 3 (2011.06.20 23HR) (LEFT : THIN SHELL MODEL, RIGHT : THE PROPOSED METHOD).....	33

FIGURE IV-VI IGP ESTIMATION ERROR RESULT OF IPP DATA 3	34
FIGURE IV-VII BAR GRAPH OF IGP ESTIMATION ERROR	38
FIGURE IV-VIII SLANT IONOSPHERIC DELAY ESTIMATION RESULT AT HIGH ELEVATION ANGLE (IRI DATA : 2011.06.20 23HR)	40
FIGURE IV-IX SLANT IONOSPHERIC DELAY ESTIMATION RESULT AT LOW ELEVATION ANGLE (IRI DATA : 2011.06.20 23HR)	41
FIGURE IV-X RMS AND MAX VALUE OF SLANT IONOSPHERIC ESTIMATION ERROR .	42

List of Tables

TABLE III-I ASSUMPTIONS USED IN THE PROPOSED METHOD.....	16
TABLE IV-I RELATION OF KP INDEX AND THE IONOSPHERE ACTIVITY.....	25
TABLE IV-II KP INDEX OF IRI DATA USED FOR VERIFICATION.....	26
TABLE IV-III MEAN OF RMS OF VERTICAL IONOSPHERIC DELAY ESTIMATION ERROR AT IPP	31
TABLE IV-IV MEAN OF RMS OF VERTICAL IONOSPHERIC DELAY ESTIMATION ERROR AT IGP (NIGHTTIME 23HR KST)	35
TABLE IV-V MEAN OF RMS OF VERTICAL IONOSPHERIC DELAY ESTIMATION ERROR AT IGP (EVENING 18HR KST)	36
TABLE IV-VI MEAN OF RMS OF VERTICAL IONOSPHERIC DELAY ESTIMATION ERROR AT IGP (DAYTIME 14HR KST).....	37
TABLE IV-VII SIMULATION CONFIGURATION FOR VERIFICATION IN USER DOMAIN...	40
TABLE IV-VIII RMS OF SLANT IONOSPHERIC DELAY ESTIMATION ERROR	43
TABLE IV-IX MAX ERROR OF SLANT IONOSPHERIC DELAY ESTIMATION ERROR.....	43

I. Introduction

1. Motivation and Objective

Global Navigation Satellite System (GNSS) is a system by which a user can point the user's location. The user uses receiver to get signals from GNSS satellite and can calculate the position using data of signals. However, there are many errors in space, such as ionospheric error, tropospheric error, satellite clock/orbit error, which make inaccuracy of estimation of the user's location[1]. A major error among them is the ionospheric error. To mitigate ionospheric errors in GNSS signal, the user can use ionospheric models such as Klobuchar or get information about ionospheric delay from a reference station. Satellite Based Augmentation System (SBAS) is also the way to reduce the error of ionosphere. SBAS generates correction data which helps user to locate user's position more precisely. One of the correction data is the ionospheric correction data. SBAS gives ionospheric correction data of Ionospheric Grid Point (IGP) and the user uses the information of IGP to calculate user's ionospheric delay. The correction data of ionospheric delay at IGP is generated with the slant ionospheric delays in signal between satellites and reference

stations. Master stations of SBAS need vertical ionospheric delays at Ionospheric Pierce Point (IPP), instead of slant delays, to calculate ionospheric correction data at IGP. Each reference station can measure the slant ionospheric delays with dual frequency, but cannot get the vertical ionospheric delays directly. As a result, reference stations have to estimate the vertical ionospheric delay and SBAS uses obliquity factor of thin shell model to get vertical ionospheric delays. However, thin shell model has some limitations. First, thin shell model assumes that peak electron density height is constant. However the peak height is high at daytime and low at night time [2]. Furthermore thin shell model does not consider spatial characteristics of ionosphere. These factors occur errors in estimation of vertical ionospheric delay from slant ionospheric delay. In this paper, we proposed a method for converting slant ionospheric delays to vertical ionospheric delay to mitigate the error of thin shell model so that the ionospheric correction of SBAS can be improved.

2. Trends of Research

To improve the accuracy of ionospheric correction, there were some former research.

There were study of different obliquity factor according to peak height of thin shell model[3].

A. Komjathy suggested a new ionospheric model which used multiple shell for Wide Area Differential GPS (WADGPS) [4]–[7]. By using multiple shell, the suggested method could consider the height variation of ionosphere that thin shell model could not. As a result, multiple shell approach showed improved SBAS ionospheric correction. However, to apply the multiple shell approach in the SBAS, SBAS has to change the current SBAS message format because it needs to send additional information compared with current SBAS process [8].

M. Hoque suggested a new method [2], [9]–[12], which can mitigate ionospheric mapping function errors [1]. The new method used Chapman profile[13] to consider vertical electron density distribution and it is assumed that vertical ionospheric delays were given. As a result, the new method showed improved estimation error in slant ionospheric delays of a user. However, the suggested method was for the improvement of SBAS user domain. If the SBAS ionospheric correction is not accurate, estimated slant ionospheric delay from the correction in the user domain can not be accurate. For this reason, it is important to generate the ionospheric correction accurately at the master station of SBAS.

In this paper, we proposed method by which ionospheric

correction can be improved, maintaining the current SBAS process.

3. Research Contents and Method

SBAS needs vertical ionospheric delays at IPP to generate ionospheric correction. Using the dual frequency, the reference station of SBAS can estimate the slant ionospheric delay. In this paper, we proposed the method to convert the slant ionospheric delay to the vertical ionospheric delay at the IPP.

The proposed method used Chapman electron density distribution [13], [14], which is a model for distribution of ionosphere. By using the Chapman profile, we could consider spatial gradient of ionosphere. The method made few assumptions. First, we assumed that the variation of ionosphere is linear. We also assumed that the vertical electron density distribution follows Chapman profile and parameters of the profile are given. To estimate the vertical ionospheric delay, we divided ionospheric into multi-layer. For the next step, vertical ionospheric delays are mapped with linear function of distance and vertical ionospheric delay at IPP. Next, we expressed segments of vertical ionospheric delays with Chapman profile. By multiplying obliquity factor to the each vertical segments and with the summation of the multiplication

results, we can express the total slant ionospheric delay with the linear equation of vertical ionospheric delay at IPP. Finally, we can obtain the vertical ionospheric delay at the IPP by solving the linear equation.

We verified the proposed method with IRI model. IRI model is a 3 dimensional empirical ionospheric model. It gives Total Electron Content (TEC) data at desired latitude, longitude and height. We calculated true ionospheric delays by integrating TEC data. Next, we estimated vertical ionospheric delays from true slant ionospheric delays by using the proposed method. Finally, we generated the ionospheric correction of SBAS with the estimated vertical ionospheric delays. For the verification, we compared estimation error of the ionospheric correction from the proposed method and from the thin shell model.

We also verified the method in the SBAS user domain. We compared the slant ionospheric delays of users with the same elevation angle through one IPP for verification in the user domain.

4. Contribution

Currently, SBAS uses a thin shell model to generate ionospheric correction. However, the thin shell model has

limitations in that it does not take into account the ionospheric vertical electron density distribution, which makes the SBAS ionospheric correction inaccurate.

In this paper, we propose the method to improve the thin shell model when estimating the vertical ionospheric delay from slant ionospheric delay. By applying the proposed method, it is possible to estimate the vertical ionospheric delay from the slant ionospheric delay more accurately than the thin shell model and consequently to improve the accuracy of ionospheric correction of SBAS. In addition, the proposed method can be applied while maintaining the current SBAS message format, which is also beneficial from a cost point of view.

As a result, this paper proposed the method to improve the SBAS ionospheric correction while maintaining the current SBAS process.

II. Current process of SBAS ionospheric correction

The SBAS consists of wide-area reference stations, wide-area master stations, uplink stations and geostationary satellites [15].

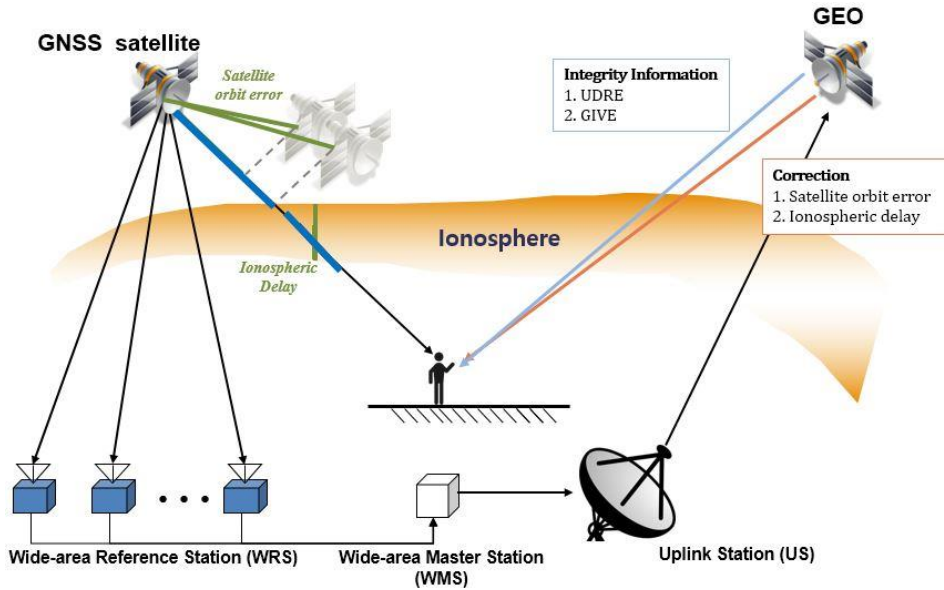


Figure II–I Conceptual figure of SBAS

The process of generating ionospheric correction in SBAS is as follows. First, the reference stations of the SBAS use dual-frequency to measure slant ionospheric delays in the signal between the GNSS satellite and the reference stations. Currently,

SBAS uses the obliquity factor of the thin shell model to estimate the vertical ionospheric delay at IPP from the measured slant ionospheric delay. The vertical ionospheric delays estimated in the reference stations are sent to the master stations. The master station generates an ionospheric correction using an algorithm called Kriging using vertical ionospheric delay at IPP. Ionospheric correction is provided to the user in the form of an Ionospheric Grid Point (IGP).

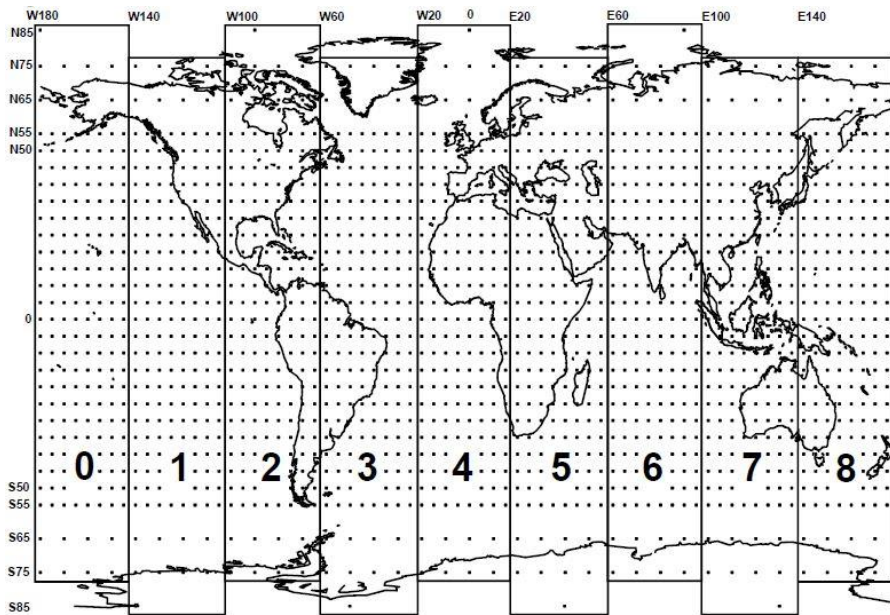


Figure II–II IGP defined in MOPS

IGP is a grid point defined in the SBAS standard document, Minimum Operational Performance Standard (MOPS). SBAS

estimates the vertical ionospheric delay in IGP and provides the information to the user. When providing the information to the user, the master station sends IGP information to the uplink station and the uplink station sends the information to the geostationary satellite. Finally, SBAS users receive IGP information from the geostationary satellite. The SBAS user receiving the IGP information uses this to calculate the vertical ionospheric delay at IPP.

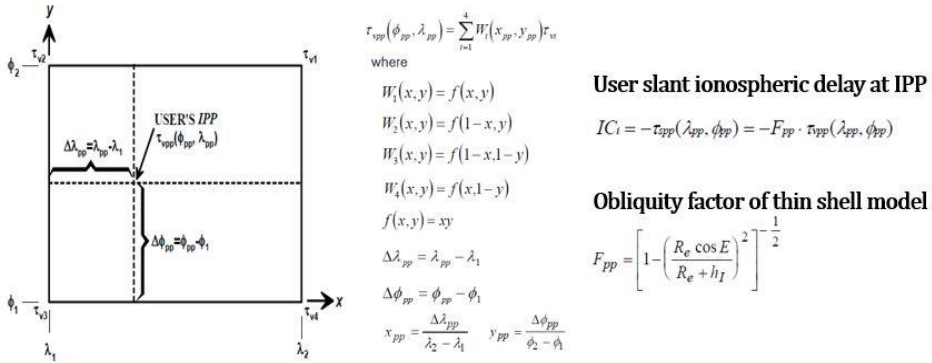


Figure II–III SBAS user algorithm of ionospheric correction

In order to estimate the vertical ionospheric delay in the IPP using the IGP information, the SBAS user follows the algorithm described in MOPS. Finally, the user calculate slant ionospheric delay between GNSS satellite and the user by multiplying obliquity factor of thin shell model to vertical delay at IPP.

Figure II–IV shows the process of applying the proposed

method to the current SBAS ionospheric correction process. The SBAS reference station uses the proposed method instead of the thin shell model to estimate the vertical ionospheric delay at IPP from the slant ionospheric delay (process ① in the figure). The master station of the SBAS then generates vertical ionospheric delays at IGP using the Kriging algorithm and sends the information to the user. The user who receives the IGP information generated by the proposed method uses the algorithm proposed by Hoque [12] rather than the thin shell model (process ② in the figure).

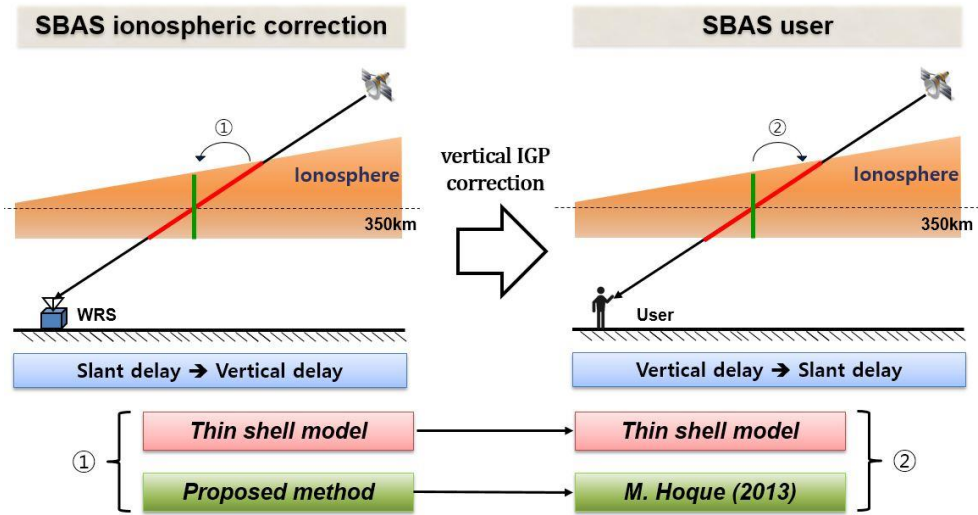


Figure II–IV SBAS ionospheric correction process with the proposed method

III. Proposed method for generation of SBAS ionospheric correction

This chapter describes the algorithm proposed in this paper. Before describing the proposed algorithm, we will briefly explain the previous studies used in the algorithm. The previous researches used are Chapman profile [13], which is a study on vertical ionospheric electron density distribution, and Hoque 's algorithm [12] which can be applied in SBAS user domain. After introducing the previous studies, the assumptions used in the proposed algorithm are described. Then, the process of the proposed algorithm is explained.

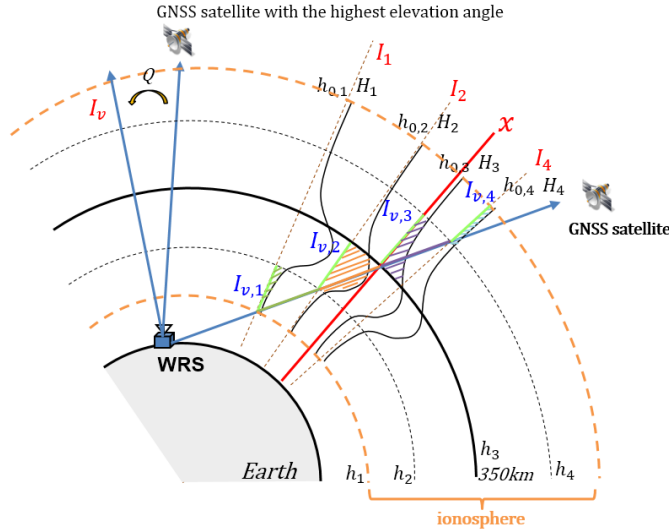


Figure III–I Conceptual figure of the proposed method

1. Introduction of Chapman profile

The Chapman profile is a model for electron density distribution of ionosphere. J. Feltens approached to 3-D global TEC representation using Chapman profile [13]. In the paper, he evaluated the profile analytically and numerically. Figure III– I shows the Chapman profile with red line and true electron density distribution of ionosphere with blue line. As can be seen, the Chapman profile follows well the trend of the true ionospheric electron density distribution.

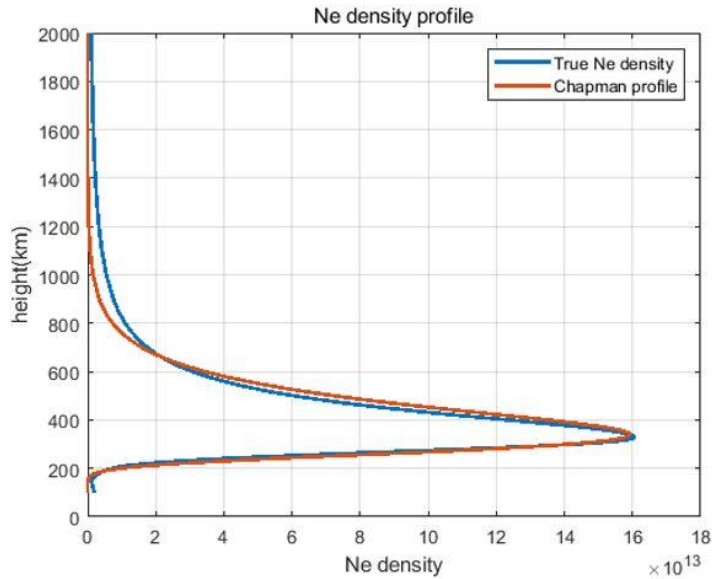


Figure III–II Chapman profile and true electron density distribution of ionosphere

$$n_e(\lambda, \phi, h) = \frac{N_0(\lambda, \phi)}{\sqrt{2\pi eH}} \exp\left(\frac{1}{2}(1 - z - \exp(-z))\right) = N_0(\lambda, \phi) \text{Chap}(h) \quad (\text{III-1})$$

$$z = \frac{h - h_0}{H} \quad (\text{III-2})$$

$$\int \text{Chap}(h) = 1 \quad (\text{III-3})$$

The above equations are those used in the Chapman profile function. λ , ϕ , h are desired longitude, latitude and height. n_e is electron density at height h , N_0 is the peak electron density, h_0 is the peak electron density altitude and H is the atmospheric scale height. The function of the Chapman profile can be determined with two parameters h_0 , H . We call these two parameters as Chapman parameters in this paper. The proposed algorithm can take into account the vertical electron density distribution of the ionosphere by using the Chapman profile and the horizontal gradient of ionospheric activity using Chapman parameters.

2. Introduction of Hoque's algorithm

M. Hoque suggested a method [12] for estimating slant ionospheric delay in signal between a user and satellites with vertical ionospheric delay. A description of the algorithm proposed

by Hoque is as follows.

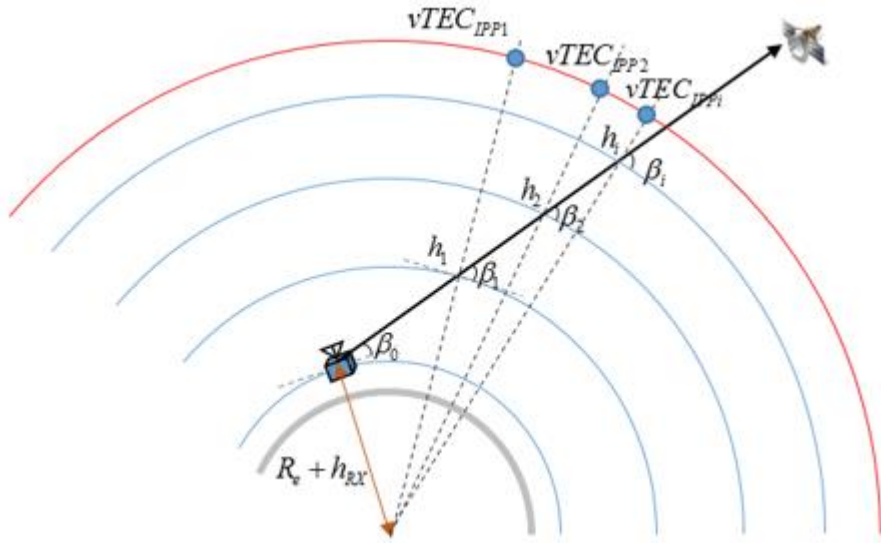


Figure III–III Conceptual figure of the Hoque's algorithm

Hoque's algorithm divides the ionosphere into several layers to estimate the slant ionospheric delay from vertical ionospheric delays. Hoque assumed that the electron density distribution of the ionosphere follows the Chapman profile and that the VTEC values of the ionosphere are known at all points. Hoque describes in his paper that VTEC values can be obtained using the SBAS. Assuming all the VTEC values are known, all the partial VTEC values for the ionosphere divided by several layers can be obtained. To obtain the slant ionospheric delay using partial VTEC values, Hoque used the following obliquity factor equation.

$$Q_i = \frac{1}{\sqrt{1 - \left(\frac{(h_i + R_e) \cos \beta_i}{h_{mIPPi} + R_e} \right)^2}} \quad (\text{III-4})$$

h_i indicates the height of the i^{th} layer of the ionosphere and R_e indicates the radius of the Earth. h_{mIPPi} means the peak electron density height of the intersection between i^{th} layer and the line of sight vector of the reference station. β_i is the elevation angle of the satellite at i^{th} layer of the ionosphere. The derivation process for the above obliquity factor equation was not described in detail in Hoque's paper. In the paper, it is assumed that the obliquity factor of the general thin shell model is used to derive the i^{th} obliquity factor (Q_i) by assigning different values to each element. However, as a result of deriving the obliquity factor, it is concluded that it is not adequate to use the obliquity factor claimed by Hoque. Therefore, this paper newly derives the i^{th} obliquity factor. The process of the derivation is explained in detail later.

The proposed method in this paper used the algorithm of Hoque as a basic idea. Hoque's algorithm was for converting vertical ionospheric delays to slant ionospheric delays. However, the process of converting slant ionospheric delays to vertical

ionospheric delays is needed to generate the ionospheric correction of SBAS. As a result, Hoque's algorithm had to be reversed. Process of reversion was not brief because of the lack of information. Finally this paper proposed method by using few assumptions, and made the algorithm for converting slant ionospheric delays to vertical ionospheric delays.

3. Assumptions used in the proposed method

In this chapter, assumptions used in the proposed method is described. The table below shows those assumptions.

Table III–I Assumptions used in the proposed method

Assumption 1	Variation of VTEC of ionosphere is linear
Assumption 2	Vertical electron density distribution of ionosphere follows the Chapman profile
Assumption 3	Chapman parameters of the profile are given

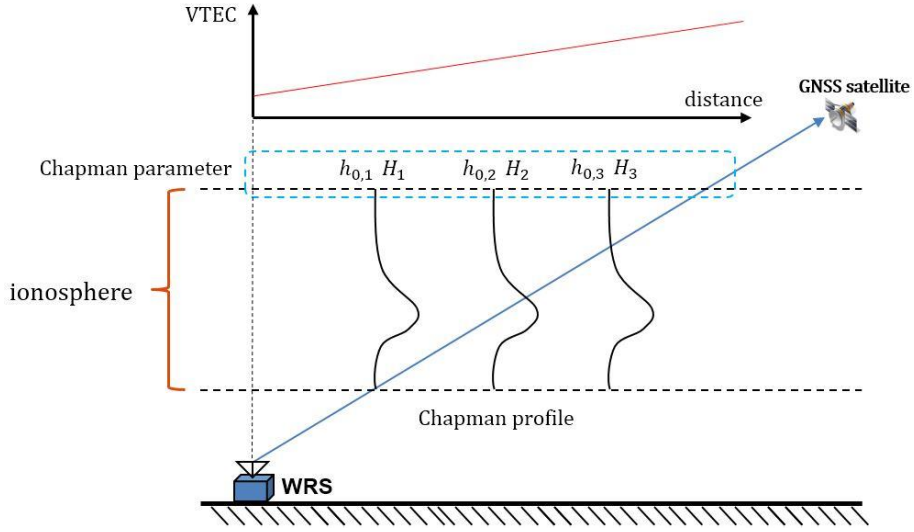


Figure III–IV Assumptions used in the proposed method

Assumption 1 was made to overcome the insufficient information when converting slant ionospheric delays to vertical ionospheric delays. As we will describe in detail the Algorithm, we can make a linear equation for vertical ionospheric delay at IPP by making this assumption. In an environment where the distance is not far and the ionosphere activity is not severe, it is safe to assume that the variation of VTEC varies linearly with distance.

Assumption 2 was made to consider horizontal gradient of the ionosphere. When the thin shell model is used, there is no way to consider the spatial characteristics of the ionosphere because the obliquity factor of the thin shell model is derived only with the geometric relationship. By assuming that vertical electron density

distribution of the ionosphere follows the Chapman profile, we can consider the peak height of electron density and vertical distribution so that we can estimate the vertical ionospheric delay at IPP more precisely.

Assumption 3 was made because Chapman parameters need to be known to use the Chapman profile. By analyzing the spatial characteristics and period of parameters, it is expected that generalized parameters can be obtained at desired point and time.

4. Development of the algorithm

Now, we will explain the proposed algorithm. The proposed algorithm is shown through Figure III–V through III–VI.

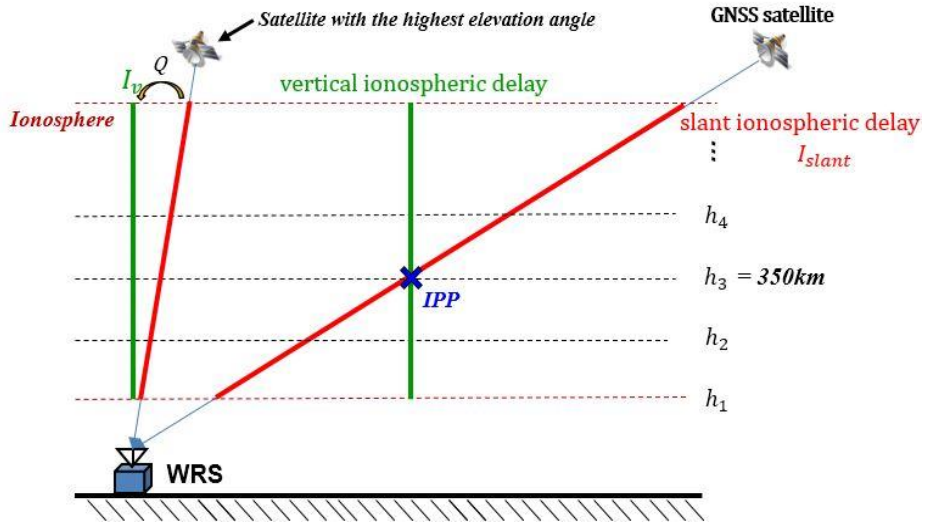


Figure III–VII Algorithm of the proposed method 1

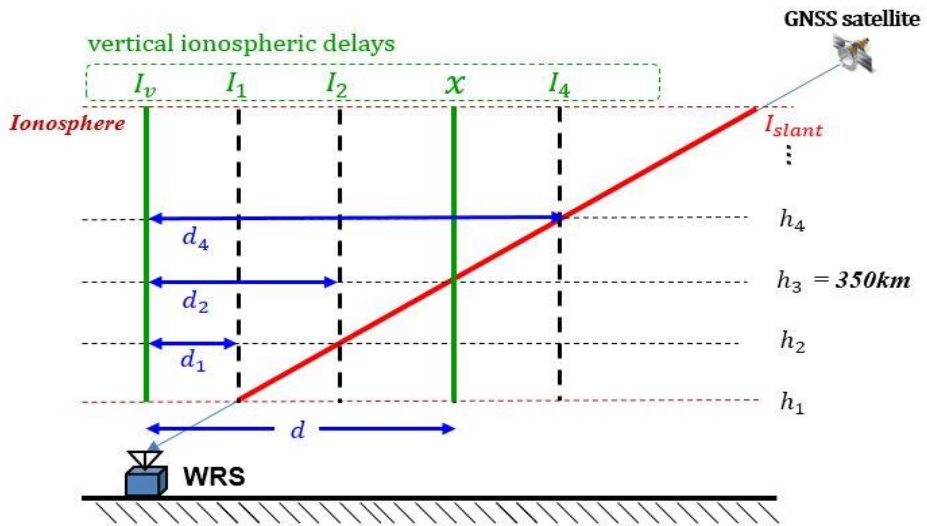


Figure III–VIII Algorithm of the proposed method 2

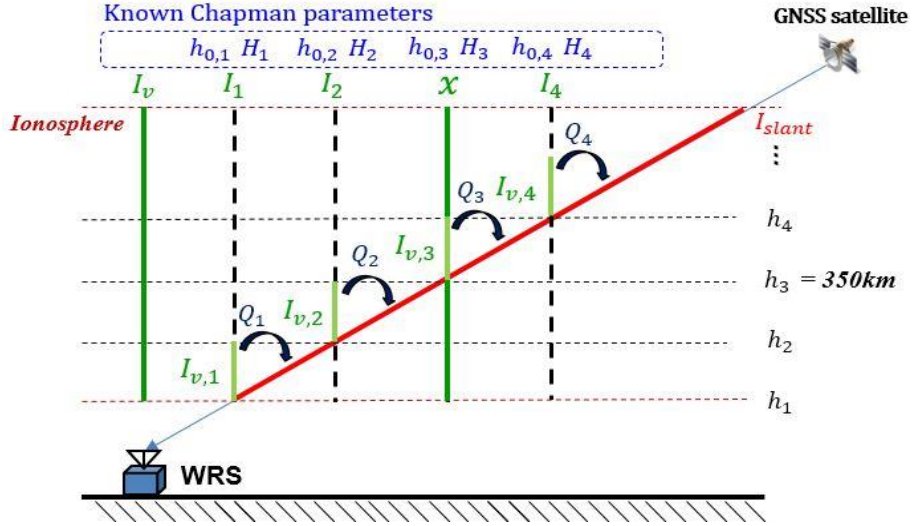


Figure III–IX Algorithm of the proposed method 3

$$I_i = (x - I_v) \frac{d_i}{d} + I_v \quad (\text{III-5})$$

$$I_{v,i} = I_i \times \int_{h_i}^{h_{i+1}} \text{Chap}(h_{0,i}, H_i, h) dh = I_i C_i \quad (\text{III-6})$$

$$I_{slant} = \sum_{i=1}^{n-1} I_{v,i} \times Q_i = f(x) \quad (\text{III-7})$$

$$Q_i = \frac{1}{\sqrt{1 - \left(\frac{(h_{RX} + R_e) \cos(\text{El})}{h_i + R_e} \right)^2}} \quad (\text{III-8})$$

$$x = \frac{I_{slant} d - ((d - d_1) C_1 Q_1 + (d - d_2) C_2 Q_2 + \dots) I_v}{d C_3 Q_3 + d_1 C_1 Q_1 + d_2 C_2 Q_2 + d_4 C_4 Q_4 + \dots} \quad (\text{III-9})$$

The final result of the proposed algorithm is the vertical ionospheric delay at the IPP between the SBAS reference station and the GNSS satellite. Therefore, we set the vertical ionospheric

delay at IPP to be unknown x .

To obtain the unknown x , the ionosphere was divided into several layers. We then used the slant ionospheric delay between the GNSS satellite with the highest elevation angle to obtain the vertical ionospheric delay at the SBAS reference stations. To estimate the vertical ionospheric delay from the slant ionospheric delay, we used the obliquity factor of the thin shell model. The reason is that the estimation error of the obliquity factor decreases as the satellite gets higher elevation angle.

In the next step, the vertical ionospheric delays of the ionosphere are mapped as a linear function of the distance and the unknown x (Equation III-5). This is possible because we assumed that the VTEC value of the ionosphere varies linearly. I_i is the vertical ionospheric delay at the junction of the i^{th} ionosphere layer and the Line Of Sight (LOS) vector between the reference station and the GNSS satellite. d is the distance between the reference station and the IPP, and the distance is calculated as 350km altitude. d_i is the distance from the reference station to the i^{th} intersection, and the altitude reference is also 350km. I_v is the vertical ionospheric delay at SBAS reference station which was obtained by using obliquity factor of thin shell model.

Next, the vertical ionospheric delay between the i^{th} layer and the $(i+1)^{\text{th}}$ layer at the i^{th} junction was expressed as Equation

III-6. This is possible because the vertical electron density distribution of the ionosphere is assumed to follow the Chapman profile. $h_{0,i}$ and H_i mean Chapman parameters at the i^{th} intersection. $I_{v,i}$ means the vertical ionospheric delay between the i^{th} layer and the $(i+1)^{\text{th}}$ layer.

In the next step, the slant ionospheric segments are obtained by multiplying each vertical ionospheric segment ($I_{v,i}$) by the i^{th} obliquity factor (Equation III-7). i^{th} obliquity factor can be derived from geometric formulas. The derivation of the obliquity factor equation is shown below.

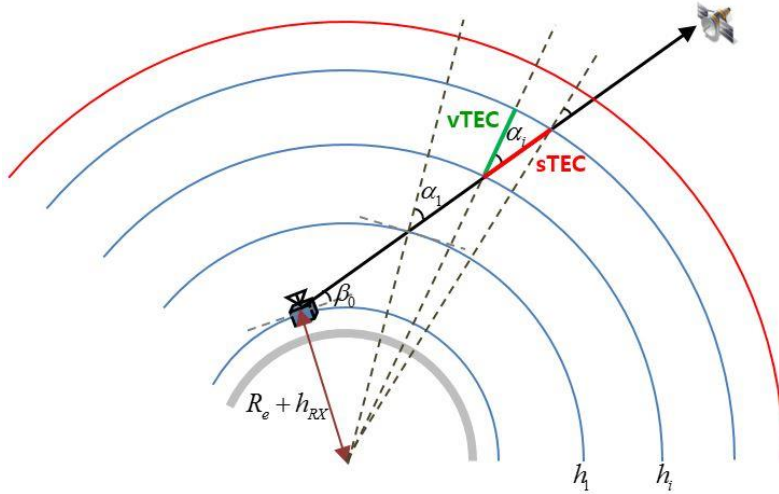


Figure III-X Derivation of i^{th} obliquity factor

$$sTEC_i^{i+1} = vTEC_i^{i+1} \times Q_i \quad (\text{III-10})$$

$$Q_i = \frac{1}{\cos \alpha_i} \quad (\text{III-11})$$

$$\frac{R_e + h_{RX}}{\sin \alpha_i} = \frac{R_e + h_i}{\sin(90 + \beta_0)} = \frac{R_e + h_i}{\cos \beta_0} \quad (\text{III-12})$$

$$\sin \alpha_i = \frac{R_e + h_{RX}}{R_e + h_i} \cos \beta_0 \quad (\text{III-13})$$

$$\cos \alpha_i = \sqrt{1 - \left(\frac{(R_e + h_{RX}) \cos \beta_0}{R_e + h_i} \right)^2} \quad (\text{III-14})$$

R_e is the radius of the earth, β_0 is the elevation angle of the GNSS satellite, h_{RX} is the height of the SBAS reference station and h_i is the height of the i^{th} ionosphere layer. The overall process of derivation is similar to the process of finding the obliquity factor of a typical thin shell model[16]. As shown above, we can obtain the i^{th} obliquity factor using Law of sines.

Finally, the total slant ionospheric delay can be expressed using vertical ionospheric delays. Since the vertical ionospheric delays were expressed as linear functions for the unknown x , the total slant ionospheric delay is also expressed as a linear function $f(x)$. Therefore, by solving the linear equation $f(x)$, we can find the vertical ionospheric delay at IPP.

IV. Verification of the proposed method

In this chapter, we will verify the proposed method. For the verification, this paper used the International Reference Ionosphere (IRI) model. IRI model is 3-D empirical model of ionosphere and it gives TEC data of desired latitude, longitude and height. We used IRI data around Korea to verify the proposed algorithm around Korea. Therefore, this paper used reference stations of Korea Augmentation Satellite System (KASS), which is a Korean SBAS. The orbits of GNSS satellites were generated using Broadcast (BRDC) and IPP data were generated with the orbits. Finally, the proposed method was verified in SBAS correction domain and the SBAS user domain.

1. Simulation for the verification

We generated environment of ionosphere by using IRI model. IRI model gives electron density, temperature, ion composition, etc. We used the electron density of IRI model. The IRI model dates were 2011.01.15, 2011.10.23, and the 20th of each month of 2011. There is K_p index which is generally recognized as indices measuring worldwide geomagnetic activity [17]. Depending on the

K_p index, the severity of the ionospheric activity can be indicated as in the following table.

Table IV–I Relation of K_p index and the ionosphere activity

K_p index	Severity of the ionosphere activity
0–2	Quiet
3	Unsettled
4	Active
5	Minor storm
6	Moderate storm
7	Strong storm
8	Severe storm
9	Extreme storm

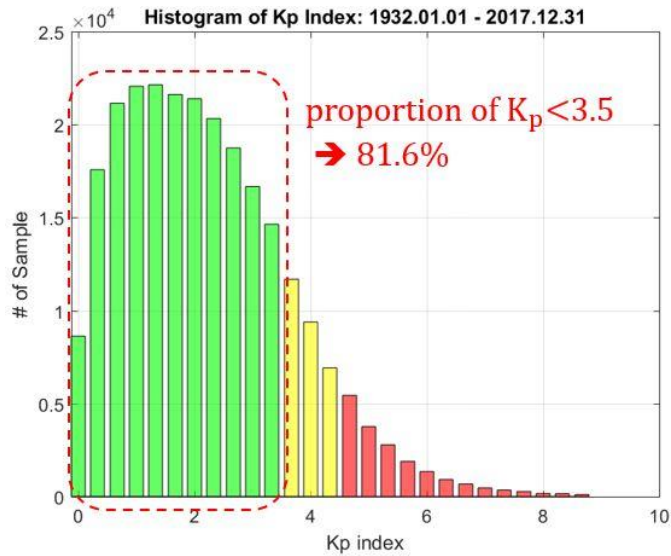


Figure IV–I Histogram of K_p index (1932.01.01 ~ 2017.12.31)

The figure above shows the histogram of the distribution of K_p index from 1932 to 2017. As a result of analysis, 81.6% of K_p index was less than 3.5. This means that most of the day's ionospheric activity is quiet or unsettled. Meanwhile, the K_p index of the 14 IRI data used in this paper is shown in the following table.

Table IV–II K_p index of IRI data used for verification

K_p index	Number of IRI data
0–2	12
3	2 (2011.04.20, 2011.07.20)
4	–
5–9	–

As shown in the table, we used a quiet and unsettled ionosphere activity environment to verify the proposed algorithm. This is because the quiet and unsettled ionosphere activity was the most prevalent in the ionospheric activity analysis, and this study is the basic study to improve the SBAS ionospheric correction. For each IRI data date, daytime (14hr), evening (18hr), and nighttime (23hr) of Korea Standard Time(KST) were used. This is to verify the proposed algorithm for various ionosphere activities. The activity of ionosphere is severe in the daytime where the solar activity is active, and the ionospheric activity becomes smaller as

it goes to the nighttime. The picture below shows the activities of the surrounding ionosphere in Korea at daytime, evening, and nighttime.

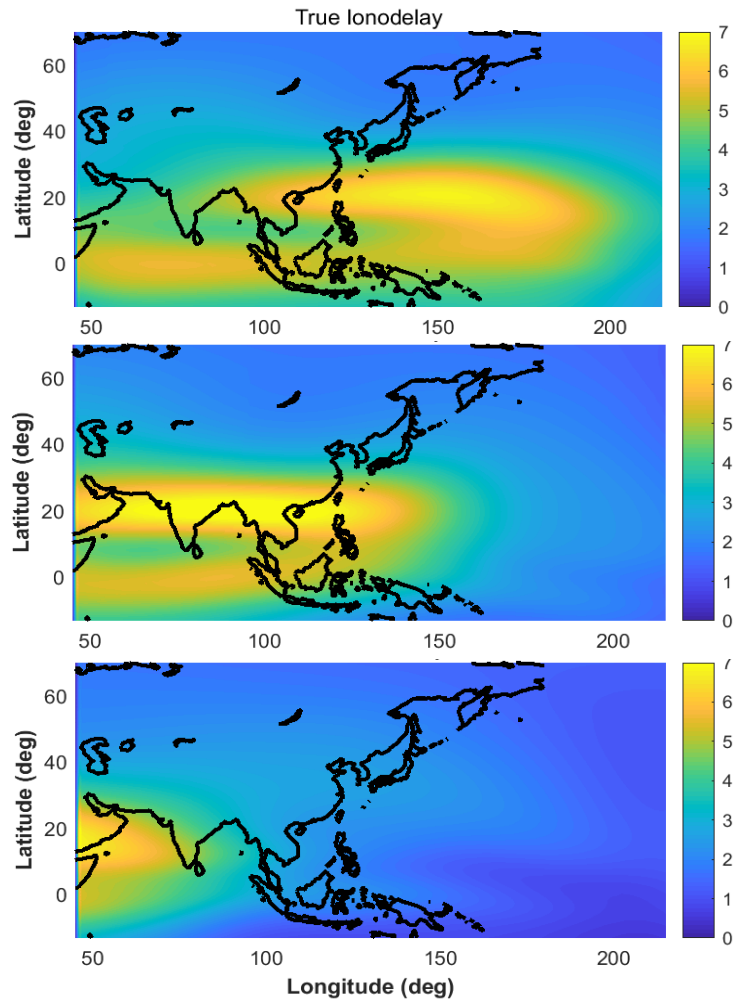


Figure IV–II Vertical ionospheric delay (m) around Korea on 2011.06.20 KST (Upper : 14hr, Middle : 18hr, Lower : 23hr)

When generating IPP data, we used reference stations of KASS, SBAS of Korea[18]. However, since KASS is under development since 2014 and has not yet been completed, we use reference stations that are currently being planned [19]. The planned location of the reference stations of the KASS is shown in the following figure.

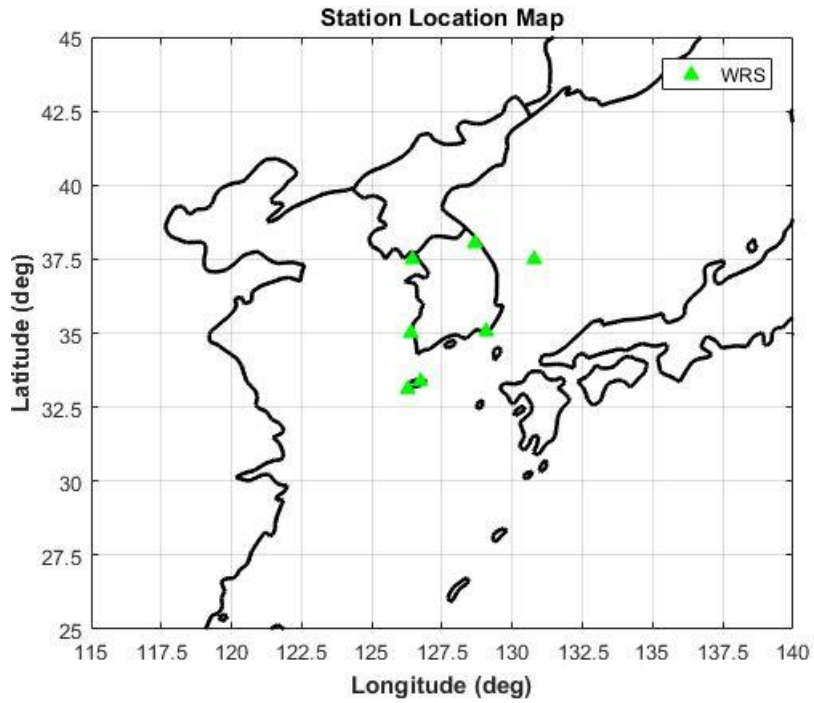


Figure IV–III Planned location of the reference stations of KASS

The orbit of GNSS satellites to generate IPP data was generated using BRDC. We used the three BRDCs, 02hr, 17hr and 22hr on 2016.08.09 (KST). This was to consider the various

placement of GNSS satellites in one ionosphere environment. We will call three IPP data as IPP data 1 through IPP data 3.

True slant ionospheric delay and true vertical ionospheric delay were obtained by directly adding TEC data from IRI data. To obtain the ionospheric delay from TEC data, the following relationship was used[20].

$$I_{true} = \frac{C_x}{2} TEC \times f^{-2} \quad (VI-1)$$

C_x is constant corresponding to the square of the plasma frequency divided by the electron density and value of $C_x/2$ is about 40.3 . f is a frequency of GNSS signal.

2. Verification in SBAS ionospheric correction domain

The results of verifying the proposed method in the SBAS ionospheric correction domain are described here. As described in Chapter II, the SBAS provides the user with an ionospheric correction in the form of a vertical ionospheric correction in the promised IGP. To generate vertical ionospheric correction in IGP, vertical ionospheric delay at IPP between reference stations and

satellite is required. Therefore, the accuracy of the estimated vertical ionospheric delay at IPP is also important. The following shows the results of the vertical ionospheric delay at IPP by using the proposed method and the thin shell model.

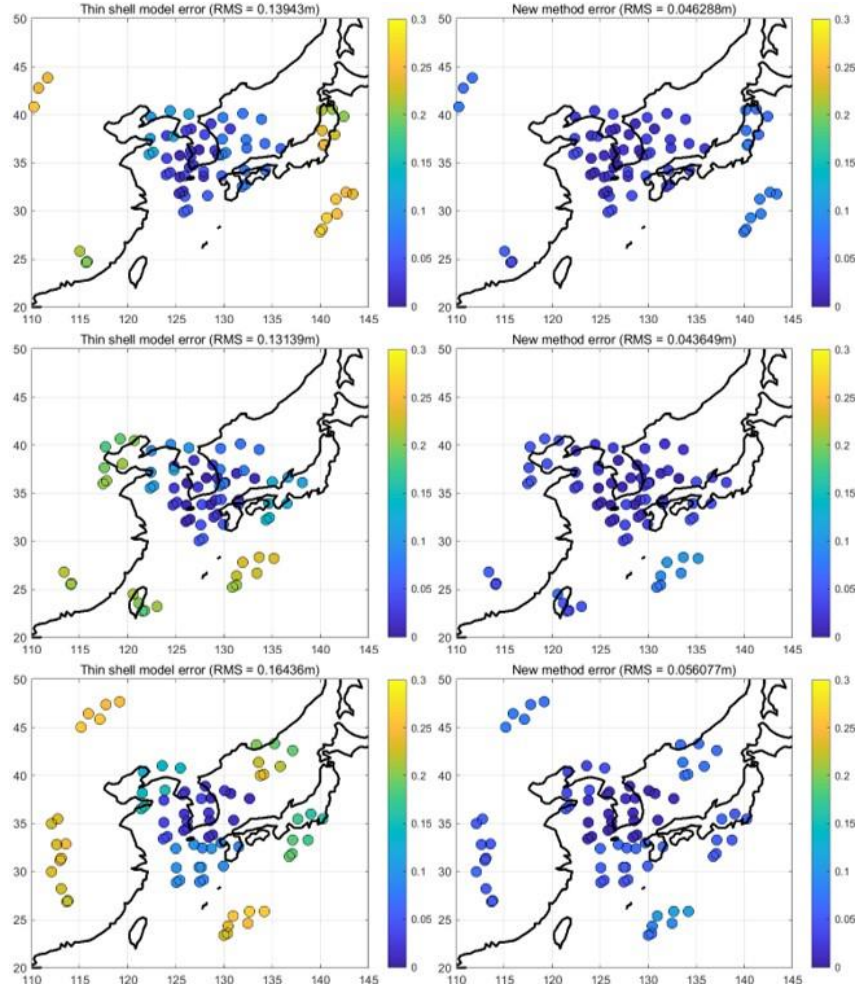


Figure IV-IV Estimation error at IPP (date : 2011.06.20 23hr)
 (left : thin shell model, right : the proposed method)
 (Upper : IPP data 1, IPP data 2, IPP data 3)

The above result shows the result of 2011.06.20 nighttime. The circles in the figure mean IPPs and the color in the circles indicates severity of the vertical ionospheric delay estimation error. The more yellow the circle is, the greater the estimation error at the IPP. Since the reference stations are located in Korea, the fact that the IPP is located outside of the map means that the IPP has a low elevation angle. As we can see in the figure, the circles in yellow when using the thin shell model, turned blue as using the proposed method. Especially, the proposed method showed improved result at IPP with low elevation angle. The table below shows the average of three IPP data result of 14 nighttime IRI data.

Table IV–III Mean of RMS of vertical ionospheric delay estimation error at IPP

# of IRI data	Thin shell model (m)	Proposed method (m)	Percentage of mitigation (%)
1	0.016	0.022	-37.5
2	0.071	0.055	22.5
3	0.018	0.024	-33.3
4	0.03	0.037	-23.3
5	0.055	0.051	7.3
6	0.094	0.029	69.1
7	0.118	0.036	69.5
8	0.145	0.049	66.2
9	0.105	0.038	63.8

10	0.089	0.029	67.4
11	0.08	0.038	52.5
12	0.073	0.056	23.3
13	0.055	0.048	12.7
14	0.039	0.043	-10.3
Mean	0.071	0.040	43.7

The proposed method showed improved result in 10 cases of 14 cases, compared with thin shell model. In case 4, estimation error was not improved but it was mm level. On the other hand, when the estimation error was improved, it improved to cm level. Finally, estimation error was improved for 43.7% when averaging the results of all IRI data.

The following is the result of generating the SBAS correction using the vertical ionospheric delay in the IPP estimated by the reference station using each method. The estimation results of IGP using the thin shell model and the proposed method are as follows.

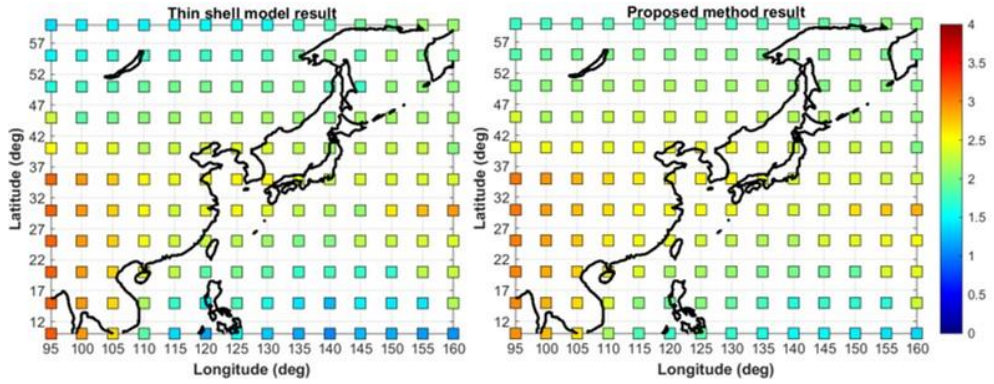


Figure IV–V IGP estimation result of IPP data 3 (2011.06.20 23hr)
(left : thin shell model, right : the proposed method)

The squares in the figure mean the IGP promised in the SBAS. Color in the square means estimated vertical ionospheric delay at IGP. To determine the estimation error, we obtained the difference between the estimated vertical ionospheric delay at IGP and the true vertical ionospheric delay at the corresponding location. The result is shown in the figure below.

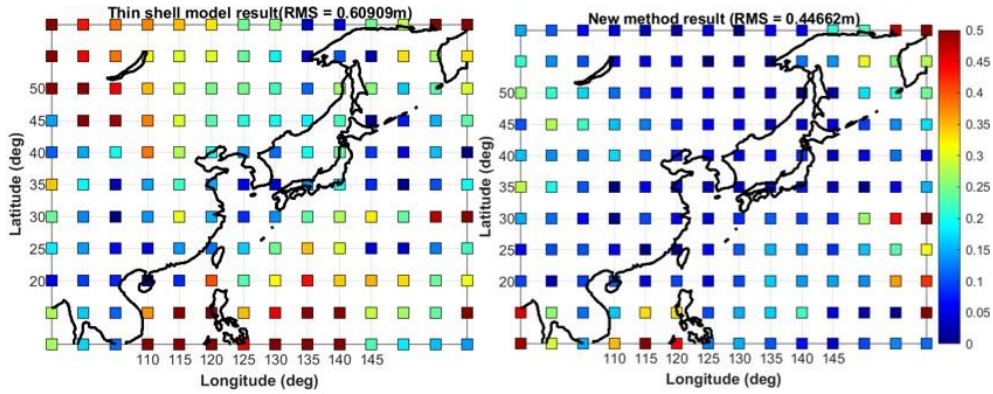


Figure IV–VI IGP estimation error result of IPP data 3
(2011.06.20 23hr)
(left : thin shell model, right : the proposed method)

In the figure above, the square also means IGP. However, the color in the square indicates severity of estimation error at IGP. The more red the square is, the greater the estimation error at the IGP. In the figure, we can see that the estimation error at IGP is reduced by using the proposed method where the estimation error was severe in the thin shell model. The table below shows the IGP estimation error results at nighttime.

Table IV–IV Mean of RMS of vertical ionospheric delay estimation error at IGP (nighttime 23hr KST)

# of IRI data	Thin shell model (m)	Proposed method (m)	Percentage of mitigation (%)
1	0.411	0.388	5.6
2	0.638	0.602	5.6
3	0.917	0.872	4.9
4	1.136	1.121	1.3
5	0.565	0.466	17.5
6	0.676	0.450	33.4
7	0.531	0.403	24.1
8	0.733	0.679	7.4
9	1.677	1.666	0.7
10	2.059	2.151	−4.5
11	1.632	1.721	−5.5
12	1.186	1.275	−7.5
13	0.400	0.377	5.8
14	2.021	2.104	−4.1
Mean	1.042	1.020	2.1

The proposed method showed improved result in 10 cases of 14 cases, compared with thin shell model. However, as a whole, the proposed method improved the RMS of the estimation error by 2.1% compared to the thin shell model. The reason for weak improvement is that the ionospheric activity is small at nighttime and therefore, the error of the thin shell model is also small.

The following table shows the result of IGP estimation error in

daytime and evening.

Table IV–V Mean of RMS of vertical ionospheric delay estimation error at IGP (evening 18hr KST)

# of IRI data	Thin shell model (m)	Proposed method (m)	Percentage of mitigation (%)
1	1.871	1.679	10.3
2	2.858	2.478	13.3
3	2.956	2.646	10.5
4	3.428	3.117	9.1
5	3.521	3.204	9
6	3.497	3.19	8.8
7	3.677	3.352	8.8
8	4.038	3.786	6.2
9	4.093	3.785	7.5
10	4.382	3.742	14.6
11	3.563	3.061	14.1
12	3.375	3.000	11.1
13	1.743	1.586	9
Mean	3.308	2.971	10.2

Table IV–VI Mean of RMS of vertical ionospheric delay estimation error at IGP (daytime 14hr KST)

# of IRI data	Thin shell model (m)	Proposed method (m)	Percentage of mitigation (%)
1	2.430	1.910	21.4
2	3.362	2.771	17.6
3	3.820	3.206	16.1
4	4.118	3.531	14.3
5	4.325	3.940	8.9
6	3.398	3.028	10.9
7	3.416	2.847	16.7
8	3.733	3.076	17.6
9	4.111	3.561	13.4
10	4.037	3.239	19.8
11	3.342	2.465	26.2
12	2.694	1.993	26
13	2.322	1.812	22
14	4.038	3.246	19.6
Mean	3.510	2.902	17.3

The proposed method showed improved result in all cases, compared with thin shell model at daytime and evening. In addition, the proposed method improved the RMS of the estimation error by 10.2% at evening and 17.3% at daytime, compared to the thin shell model. For a clear view, we drew the bar graph of the results in the table above.

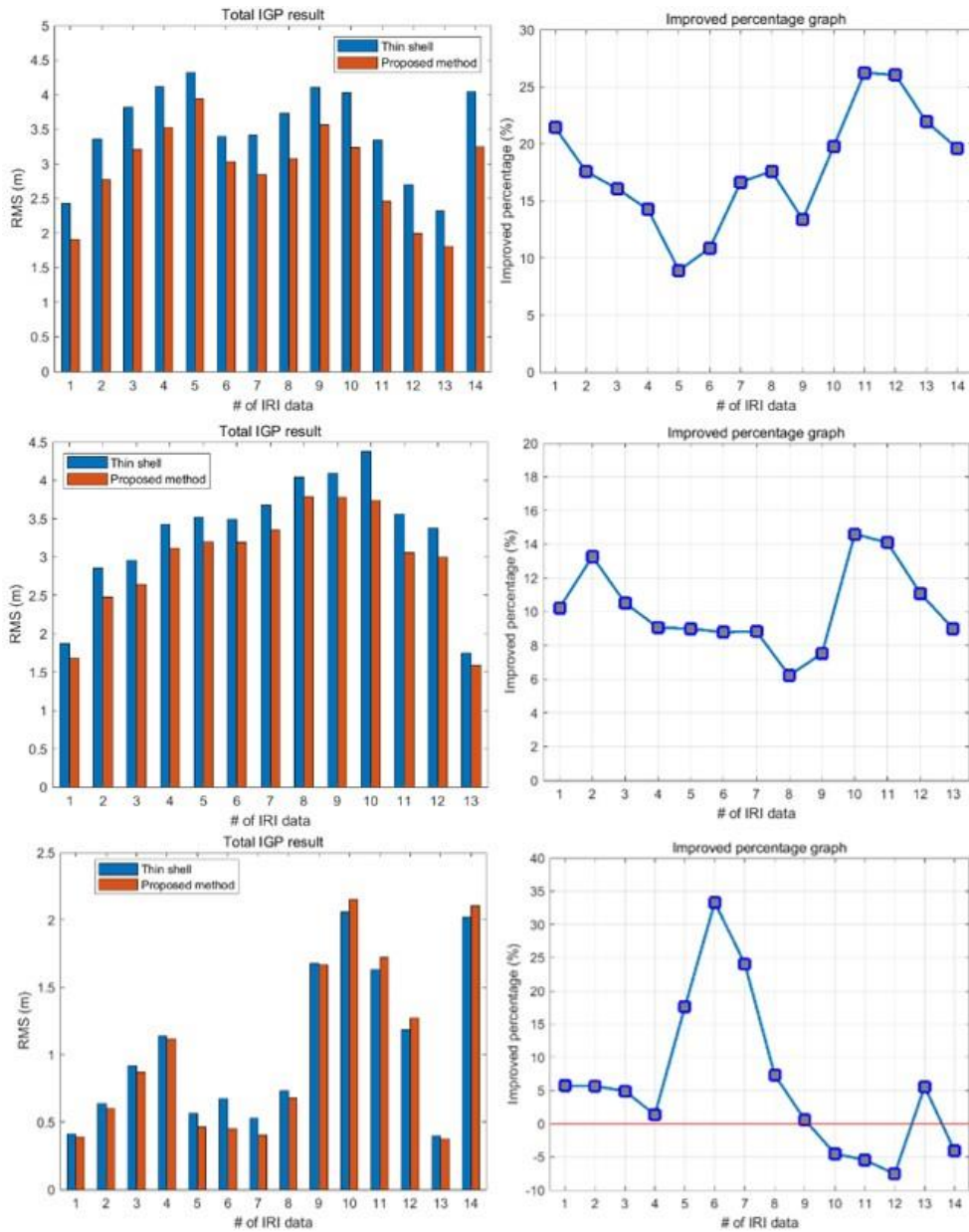
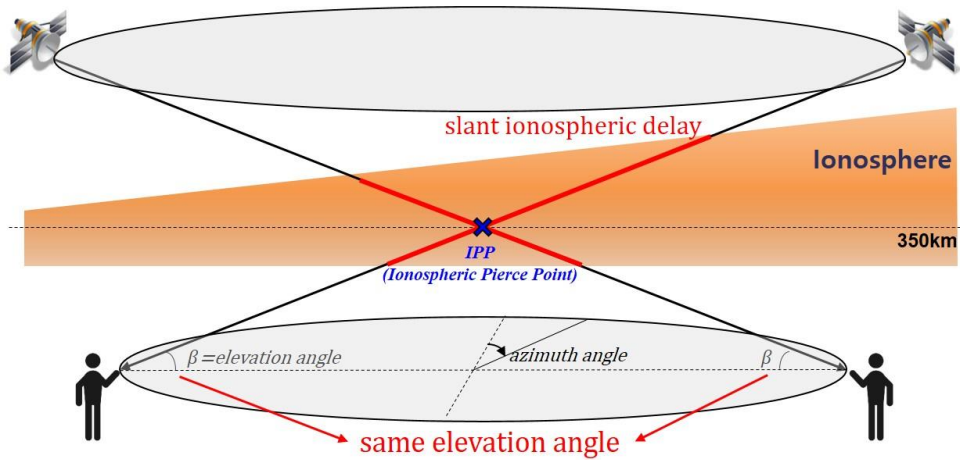


Figure IV–VII Bar graph of IGP estimation error
(Upper : daytime, Middle : evening, Lower : nighttime)

3. Verification in SBAS user domain

The previously generated SBAS correction was verified in the user domain. When verifying the proposed method in the user domain, we compared slant ionospheric delay values for users whose LOS vector from the satellite penetrates the same IPP with the same elevation angle. Conceptual figure of the method of verification in user domain is below.



Slant ionospheric delay was obtained by using the previously generated SBAS correction. As described in Chapter II, the SBAS ionospheric correction generated by the thin shell model was applied to the user domain using a thin shell model whereas the algorithm of Hoque [12] was used to apply the proposed method to the user domain. The following table shows the simulation

configuration for verifying the proposed method in the user domain.

Table IV–VII Simulation configuration for verification in user domain

Contents	Value
IPP Location	latitude : 37deg longitude : 127deg
User azimuth angle	0 ~ 360deg (10deg interval)
User elevation angle	10 ~ 70deg (10deg interval)

The following figure shows the result of the estimated slant ionospheric delay according to the user's azimuth angle.

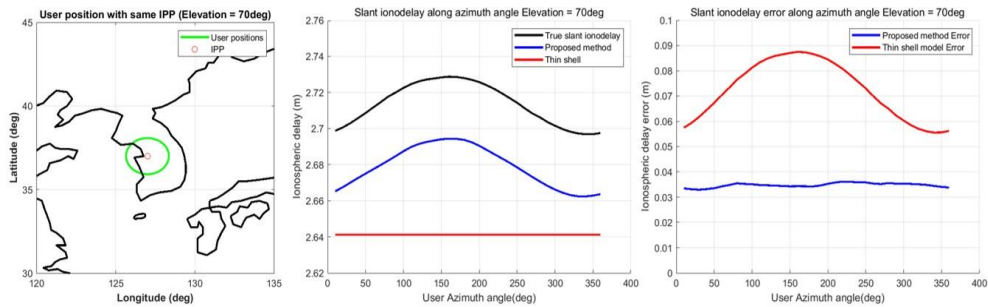


Figure IV–VIII Slant ionospheric delay estimation result at high elevation angle (IRI data : 2011.06.20 23hr)

(Left : location of IPP and user, Middle : slant ionospheric delay, Right : estimation error)

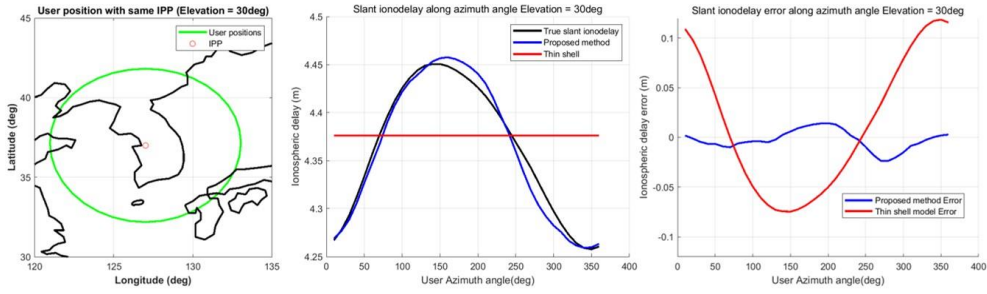


Figure IV–IX Slant ionospheric delay estimation result at low elevation angle (IRI data : 2011.06.20 23hr)

In the middle graphs, the slant ionospheric delay obtained by using the proposed method (blue line) follows well the tendency of true slant ionospheric delay both in low and high elevation angle. However, in the case of the thin shell model, the slant ionospheric delay is assumed to be constant because the function of the obliquity factor depends only on the elevation angle. To numerically determine whether the results of each method follow the trend well, the RMS of error and max error value were compared according to the elevation angle. Finally, the results of estimation errors of slant ionospheric delays were derived for all IRI data. The figure below shows the RMS and max value of estimation error according to the elevation angle.

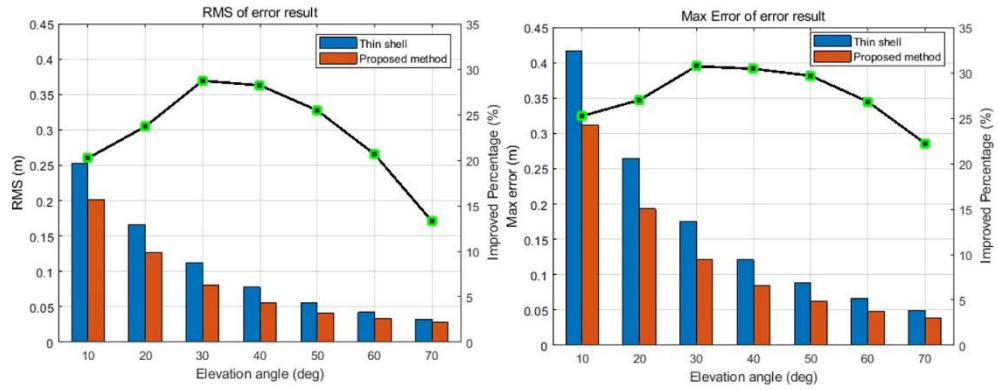


Figure IV–X RMS and max value of slant ionospheric estimation error

The smaller the elevation angle, the larger the RMS and max value are because the LOS vector passes through the ionosphere more. For all elevation angles, using the proposed method, the RMS and max value are reduced compared to the thin shell model. Specific values of the figure are summarized in the following table.

Table IV–VIII RMS of slant ionospheric delay estimation error

Elevation angle (deg)	Thin shell model (m)	Proposed method (m)	Percentage of mitigation (%)
10	0.253	0.201	20.6
20	0.167	0.127	24.0
30	0.113	0.080	29.2
40	0.078	0.056	28.2
50	0.056	0.042	25.0
60	0.042	0.033	21.4
70	0.033	0.028	15.2
Mean	0.106	0.081	23.6

Table IV–IX Max error of slant ionospheric delay estimation error

Elevation angle (deg)	Thin shell model (m)	Proposed method (m)	Percentage of mitigation (%)
10	0.416	0.311	25.2
20	0.265	0.193	27.2
30	0.175	0.121	30.9
40	0.121	0.084	30.6
50	0.089	0.063	29.2
60	0.066	0.048	27.3
70	0.049	0.038	22.4
Mean	0.169	0.123	27.2

On average, the proposed method improved RMS by 23.6% and max by 27.2%.

V. Conclusion

In this paper, we proposed the method to improve accuracy of the SBAS ionospheric correction. What is needed to generate the SBAS ionospheric correction is the vertical ionospheric delay at IPP, but the estimated value at the reference stations is the slant ionospheric delay. Therefore, we need to estimate vertical ionospheric delay from slant ionospheric delay accurately, and this paper focused on this part.

The proposed method considers the spatial gradient of the ionosphere using the Chapman profile. It was assumed that the VTEC of ionosphere varies linearly and Chapman parameters are given. Finally, by dividing the ionosphere into multi-layer, vertical ionospheric delay was estimated from slant ionospheric delay.

We verified the method both in the SBAS ionospheric correction domain and the SBAS user domain, As a result, the proposed method improved SBAS ionospheric correction for 17.3% in daytime, 10.2% in evening, 2.1% in nighttime. In SBAS user domain, slant ionospheric delay result of the proposed method followed the tendency of true result. For numerical result, RMS and max value of estimation improved for 23.6% and 27.2% when the proposed method used.

This paper also contributed at the point that the current SBAS

message format does not need to be changed, when applying the proposed method. For the future work, the proposed method have to be verified in the severe ionospheric environment. If the verification results are accurate, it is possible to apply the proposed method to the actual SBAS after additional verification.

Reference

- [1] B. P. Misra and P. Enge, "Global Positioning System : Signals , Measurements and Performance Second Edition," 2005.
- [2] M. M. Hoque, N. Jakowski, and J. Berdermann, "A new approach for mitigating ionospheric mapping function errors," *27th Int. Tech. Meet. Satell. Div. Inst. Navig. ION GNSS 2014*, vol. 2, 2014.
- [3] Z. Huang and H. Yuan, "Analysis and improvement of ionospheric thin shell model used in SBAS for China region," *Adv. Sp. Res.*, vol. 51, no. 11, pp. 2035–2042, 2013.
- [4] A. Komjathy *et al.*, "A New Ionospheric Model for Wide Area Differential GPS : The Multiple Shell Approach," *Network*, no. January, pp. 28–30, 2002.
- [5] D. Kim, D. Han, H. Yun, and C. Kee, "Performance Improvement of Grid Ionospheric Delay Correction Based on Multiple Constellations for Single–Frequency SBAS User."
- [6] A. L. Tao and S. S. Jan, "Wide–area ionospheric delay model for GNSS users in middle– and low–magnetic–latitude regions," *GPS Solut.*, vol. 20, no. 1, pp. 9–21, 2016.
- [7] K. N. S. Rao, "GAGAN – The Indian satellite based augmentation system," vol. 36, no. August, pp. 293–302, 2007.
- [8] L. Sparks, B. A. Iijima, A. J. Mannucci, and B. D. Wilson, "A New Model for Retrieving Slant Corrections for Wide Area Differential GPS," *Jet Propuls. Lab.*, no. January, pp. 26–28, 1999.
- [9] N. Jakowski, M. M. Hoque, and C. Mayer, "A new global TEC model for estimating transionospheric radio wave propagation errors," *J. Geod.*, vol. 85, no. 12, pp. 965–974, 2011.
- [10] M. M. Hoque and N. Jakowski, "A new global model for the ionospheric F2 peak height for radio wave propagation," *Ann. Geophys.*, vol. 30, no. 5, pp. 797–809, 2012.
- [11] M. M. Hoque and N. Jakowski, "A new global empirical NmF2 model for operational use in radio systems," *Radio Sci.*, vol. 46, no. 6, 2011.
- [12] M. M. Hoque and N. Jakowski, "Mitigation of ionospheric mapping function error," *Proc. 26Th Int. Tech. Meet. Satell.*

- Div. Inst. Navig. (Ion Gnss 2013)*, pp. 1848–1855, 2013.
- [13] J. Feltens, F. D. Division, E. Space, and O. Centre, “CHAPMAN PROFILE APPROACH 3–D GLOBAL TEC REPRESENTATION.”
 - [14] S. C. Mushini, P. T. Jayachandran, R. B. Langley, and J. W. MacDougall, “Use of varying shell heights derived from ionosonde data in calculating vertical total electron content (TEC) using GPS – New method,” *Adv. Sp. Res.*, vol. 44, no. 11, pp. 1309–1313, 2009.
 - [15] D. Kim, “A Study on correction generation algorithms for wide area differential GNSS,” Ph. d. thesis, Seoul national university, 2007.
 - [16] N. Yaacob, M. Abdullah, and M. Ismail, “GPS Total Electron Content (TEC) Prediction at Ionosphere Layer over the Equatorial Region,” *Trends Telecommun. Technol.*, 2010.
 - [17] A. Dessler and J. Fejer, “Interpretation of K p index and M–region geomagnetic storms,” *Planet. Space Sci.*, vol. 11, pp. 505–511, 1963.
 - [18] E. Bang, J. Lee, J. Lee, and T. Walter, “Constructing Ionospheric Irregularity Threat Model for Korean SBAS,” *Proc. ION GNSS Conf. 2013*, pp. 296–306, 2013.
 - [19] T. Authié *et al.*, “Performances Monitoring and Analysis for KASS,” pp. 958–978, 2015.
 - [20] M. B. Katta, R. Priyakanth, and T. Kunam, “A Systematic Study of ‘ Estimation of Ionospheric Delay Errors in GPS ,”” vol. 7, no. 1, pp. 97–101, 2017.

초 록

SBAS(Satellite Based Augmentation System)은 GNSS(Global Navigation Satellite System) 사용자에게 전리층 보정 정보를 제공함으로써 사용자로 하여금 자신의 위치를 정확하게 추정할 수 있도록 한다. 전리층 보정 정보를 생성하기 위해 SBAS의 기준국에서는 경사 전리층 지연 값으로부터 IPP(Ionospheric Pierce Point)에서의 수직 전리층 지연 값을 추정하며 이 때 thin shell model의 obliquity factor를 이용한다. 하지만 obliquity factor는 단순히 위성 양각에 따른 함수이다. 따라서 수직 전리층 지연 값이 부정확하게 추정되고 이로 인해 전리층 보정 정보 역시 부정확하게 생성이 된다.

본 논문에서는 SBAS 전리층 보정 정보의 정확성을 높이기 위해 경사 전리층 지연 값으로부터 수직 전리층 지연 값을 추정하는 새로운 방안을 제안하였다. 제안한 방안은 전리층의 수직 전자 밀도 분포를 모델링한 Chapman profile을 이용하였다. 이 때 Chapman profile의 parameter들은 주어졌고 거리에 따른 전리층 활동이 선형이라고 가정하였다. 또한 전리층을 여러 층으로 나누어 경사 지연 값으로부터 수직 전리층 지연 값을 구하였다.

검증 방안으로는 제안한 방법을 이용하여 수직 전리층 지연 값을 추정하고 그 값을 이용해 SBAS 전리층 보정 정보를 생성하였다. 이 때 검증을 위한 시뮬레이션 데이터로는 IRI(International Reference Ionosphere) 모델을 사용하였다. 결과적으로 제안한 방법을 이용해

전리층 보정 정보를 생성했을 때 thin shell 모델에 비해 정확도가 낮 시간의 경우 17.3%, 저녁 시간의 경우 10.2%, 밤 시간의 경우 2.1% 개선되는 것을 확인하였다. 또한 생성한 보정 정보를 이용해 SBAS 사용자의 경사 전리층 지연 값을 구하고 그 결과를 비교하였다. 이 경우 제안한 방법의 경사 전리층 지연 추정 오차가 thin shell 모델에 비해 RMS 는 23.6%, 최대 오차 값은 27.2% 감소한 것을 확인하였다.

주요어 : SBAS, 전리층 보정 정보, Chapman profile, 전리층 지연, IRI

학 번 : 2017-20877